

## AN INTEGRATED FRAMEWORK FOR THE RELIABILITY AND VALIDITY ASSESSMENT OF NUMERICAL WIND ENGINEERING SIMULATIONS

AHMED ABODONYA\*, JORDI COTELS<sup>†</sup>, ROLAND WÜCHNER\* AND  
KAI-UWE BLETZINGER\*

\* Chair of Structural Analysis  
Technical University of Munich  
Arcisstr. 21, D-80333 München  
e-mail: ahmed.abodonya@tum.de - Web page: <http://www.st.bgu.tum.de>

<sup>†</sup> CIMNE - Centre Internacional de Metodes Numerics en Enginyeria  
Universitat Politècnica de Catalunya  
Campus Norte UPC, 08034 Barcelona, Spain  
e-mail: jcotela@cimne.upc.edu, web page: <http://www.cimne.com/>

**Key words:** Simulation Reliability, Code Verification, CWE, KRATOSMultiphysics

**Abstract.** Towards complex architecture and light-weight structures, conventional wind load estimation techniques fail. Hence, Computational Wind Engineering (CWE) plays a crucial role. CWE can be a very helpful tool in all design stages from schematic to detailed design stage. With the current advances in CWE, numerical wind tunnel simulations has a great potential towards improving the structural design quality through better understanding of the wind loads on structures. However, the quality of simulations is still questionable. Despite the increasing attention given to the quantification of error and uncertainty in CFD, the techniques that have been developed for general fluid engineering problems to assess the quality of CFD simulations are still marginally used in CWE (Jrg Franke, 2010). This paper is part of a project aiming at defining a framework to assess the predictive capability of wind load computation using CWE with error estimation. The framework consists of three main work packages: Code Verification, Solution Verification, and Validation. Overall, the generic definition of the framework is stepwise exemplified with the open-source code KRATOSMultiphysics. In this paper, Code Verification is the main concern. The Method of Manufactured solutions is used to verify the Variational Multiscale (VMS) element in KratosCFD incompressible Navier-Stokes solver. Taylor-Green vortex is the basis for the verification test. The Taylor-Green vortex is a well-studied test problem for large eddy simulation (LES) subgrid scale models. Moreover, Taylor-Green vortex is modified to have more extensive testing for the code. Finally, a second order convergence rate is observed which verifies the tested code functionality, then numerical errors are to be quantified.

## 1 INTRODUCTION

In today's world, societal needs have led to the wide spread of tall buildings and large span light weight structures. Limited spaces and modern architectural features are imposing challenges to designers of tall and super-tall buildings. Consequently, emphasis is added on safety, human comfort and serviceability under wind loading. These considerations together with geometrically complex shapes have led to two main challenges for the designers. Firstly, the wind loading assessment on such structures is very complex using experimental approaches which raises the attention towards computational analysis. Secondly, the high aerodynamic loads acting on the structures lead to the usage of more materials. Consequently, both the computational wind loading assessment on structures and the reduction of aerodynamic loads are of crucial impact on having optimal building design. Furthermore, information on the wind loads can be obtained through the physical modelling of Fluid-Structure Interactions (FSI). Recently, FSI in Computational Wind Engineering (CWE) is gaining confidence and is widely used in aerospace and mechanical engineering applications. From [3] and [4], it was concluded that the accuracy of both wind tunnel testing and CWE is questionable. Therefore, it can be safely said that both methods need some error indicators to increase their reliability. Consequently, the need for a quality assessment approach in CWE is raised and is the subject of this project. This project aims at developing an integrated methodology that is used in the assessment of simulation predictive quality. The development will be robust and software independent. These tools are envisaged as fundamental contributions for the development of an integrated framework for a reliable wind loads prediction.

## 2 ASSESSMENT FRAMEWORK

The proposed framework shown in figure 1 is a sequential evaluation for the simulation quality. Code verification, solution verification and validation are the main building blocks for the assessment procedures.

### 2.1 Code verification

This part of the process is essential to the process of having a reliable simulation. Code verification is defined in [5] as "The process of determining that the numerical algorithms are correctly implemented in the computer code and of identifying errors in the software". In the context of this paper, code verification is performed using the method of exact solution (MES) as a base, then more sophisticated approach is developed using the method of manufactured solution (MMS). The flowchart in figure 1 shows the important steps to follow in order to have a meaningful code verification campaign. Moreover, section 3 shows a detailed case study for the proposed code verification approach.

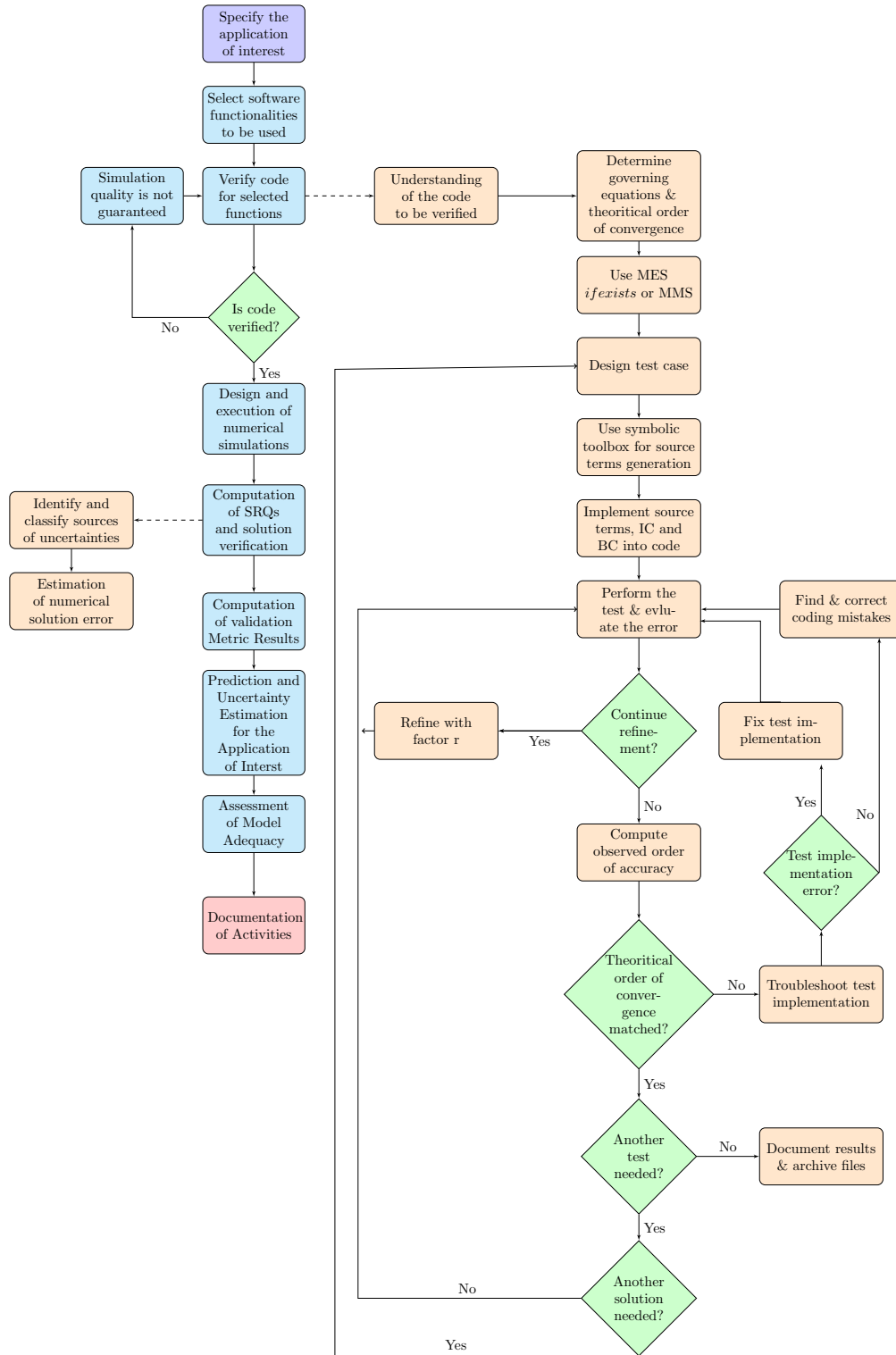


**Figure 1:** Flowchart for the integrated procedure for V&V adapted from [6], [8], [7]

## 2.2 Solution verification

Solution verification is defined in [5] as "The process of determining the correctness of the input data, the numerical accuracy of the solution obtained, and the correctness of the output data for a particular simulation". It addresses the quantification of error originating from human intervention and numerical errors. In the scope of this paper, this part of the process is under development where it will be designed to deal with unsteadiness in the flow field.

## 2.3 Computation of validation metric results

Graphical comparisons between simulations and experiments are not considered sufficient to judge the quality of CWE simulations. For a sufficient validation process, code correctness must be checked as of code verification. Moreover, simulation error is to be quantified as of solution verification. Then, the validation process can be completed as described in [1] and [2].

## 3 PROBLEM SETUP FOR KratosCFD CODE VERIFICATION

In this section, code verification activities are presented for KratosCFD [9] open source code. The formulation for tested functionalities and code implementation can be found in [10] and [11]. The code verification activities performed are based on the Taylor-Green Vortex. In the context of this work only 2D Navier-Stokes equations for an incompressible Newtonian fluid is considered. The testing activities have an increasing complexity starting from an equal contribution of all the terms in the Navier-Stokes equations to a term dominating solution. The following benchmark series is developed based on the Taylor-Green Vortex to test each term in the Navier-Stokes Equations. This is done for the purpose of exploring which term is affecting the code order of convergence and needs more investigation in case of unclear convergence. The approach is through giving the term of interest very high weight compared to others in the N-S in which the error generated from this term will be the dominating error.

### 3.1 Taylor-Green Vortex (TGV)

The Taylor-Green vortex is an exact closed form solution of the incompressible N-S equations. It is an unsteady flow of a decaying vortex. The solution is a periodic array of vortices that repeats itself in two Cartesian dimensions. Detailed description of the TGV can be found in [12] and [13]. The general form of the Taylor-Green Vortex is defined as following:

$$u_x = u_0 f(t) \sin(kx) \cos(ky) \quad (1)$$

$$v_y = -u_0 f(t) \cos(kx) \sin(ky) \quad (2)$$

$$Pr = \frac{\rho u_0^2}{4} f(t)^2 (\cos(2kx) + \sin(2ky)) \quad (3)$$

Where:

$$f(t) = e^{-2\nu k^2 t}; \nu \rightarrow \text{kinematic viscosity} \quad (4)$$

$$k = \frac{2\pi}{L}; L \rightarrow \text{Periodic Length}; \rho \rightarrow \text{Density} \quad (5)$$

$$\text{Reynolds number: } Re = \frac{Lu_0}{\nu} \quad \text{Courant number: } CFL = \frac{u_0 \Delta t}{\Delta x} \quad (6)$$

### 3.2 Overview for KratosCFD Tested Functionalities

In the course of this work KratosMULTIPHYSICS FEM based solver, developed at CIMNE, is to be verified. The code is claimed to have a second order convergence in space and time. The actual order of convergence of the following functionalities is to be verified:

Finite Element Method
Steady State
Unsteady using WBZ- $\alpha$ (Bossak)
Incompressible Fluid
VMS Monolithic Solver
Orthogonal Subscales Stabilization

### 3.3 Calculation of the error and order of convergence

The numerical solution consists of values of the dependent variables on some set of discrete locations. To compute the discretization error, two error norms are used. Error norms can be used to determine the global error of a field  $\mathbf{b}$  in its spatial domain  $K$ . An  $E_2$  error norm for the variable  $\mathbf{x}$  compared to the exact solution  $\hat{\mathbf{x}}$  in the domain  $\mathbf{K}$  can be seen in equation 7.

$$E_2 = ||\mathbf{x} - \hat{\mathbf{x}}||^2 = \sqrt{\frac{1}{K} \int_K (\mathbf{x} - \hat{\mathbf{x}})^2 dK} \quad (7)$$

Moreover, the infinity (inf) norm returns the maximum absolute error over the entire domain given by equation 8. Therefore, it is the most sensitive error measure. It is very proper to detect local discontinuities or singularities.

$$E_i = \max |x_n - \hat{x}_n|, \quad n \in [1, N] \quad (8)$$

After error evaluation and simulating over several meshes, the information is used to estimate the observed order-of-convergence. The observed order-of-convergence is estimated using the expression shown in equation 9.

$$p = \frac{\log \left( \frac{E(h_{coarse})}{E(h_{fine})} \right)}{\log(r)} \quad (9)$$

### 3.4 Simulation setup

1. Spatial and temporal resolutions:

Kratos uses triangular elements in which meshes can be designed in three ways:

- Unidirectional Structured Mesh
- Alternate Diagonal Structured Mesh
- Unstructured Mesh

In the scope of the results presented below, unidirectional structured mesh is considered. The extension to unstructured mesh is the most crucial because it is the most commonly used mesh type in Kratos. Consequently, the behavior of the code for unstructured meshes is of high interest. Both Reynolds number and Courant number are considered while deciding on the spatial and temporal resolution. CFL number is kept below one for all the simulations. The refinement ratio in both space and time is 2 which complies with the code's theoretical order of convergence.

2. Dirichlet boundary condition is used for both velocity and pressure terms in all the boundaries, because our target is the verification of the interior equations.
3. The discretization error should be isolated from the total numerical error. Therefore, the used software is using a double precision accuracy to minimize the round-off error. To keep the IICE as small as possible, the solution tolerance in a non-normalized version of the  $E_2$  norm of velocity and pressure fields is set to  $10^{-10}$ .
4. A direct solver is used for solving the linear system of equations.
5. The basic setup for the simulations is declared in table 1.

**Table 1:** Basic simulation setup declaration

<b>Mesh Type:</b>	Unidirectional Structured Mesh
<b>Element:</b>	VMS Monolithic Solver
<b>Linear System Solver:</b>	Super LU "Direct Solver"
<b>Domain size:</b>	$X_1 = x \in [0, 2\pi], X_2 = y \in [0, 2\pi], t \in [0, 10]$
<b>Space Refinement (SR):</b>	Space (cells/direction): $2^{2^{\frac{\text{increment}}{1}} \rightarrow 8}$ , $\Delta t = 0.001$
<b>Time Refinement (TR):</b>	Space (cells/direction): $2^8$ , $\Delta t = 2^{1^{\frac{\text{increment}}{1}} \rightarrow 7} 10^{-3}$
<b>Space-Time Refinement (STR):</b>	Space (cells/direction): $2^{2^{\frac{\text{increment}}{1}} \rightarrow 8}$ , $\Delta t = 2^{7^{\frac{\text{decrement}}{1}} \rightarrow 1} 10^{-3}$

---

## 4 BENCHMARKS

In this section all the benchmarks will be defined in tables 2 and 3.

**Table 2:** Base Benchmark

Test Case	Fields	Material	Source Terms	Discretization
TGV1	Using the general form of the	$\nu = 0.2$	NO	SR
TGV2	Taylor-Green Vortex with	$\rho = 1.0$		TR
TGV3	parameters: $k = 1.0$ , $u_0 = 1.0$			STR

**Table 3:** Developed Benchmarks

Test Case	Fields	Material	Source Terms	Discretization
IN1	$u_x = \sin(t)$	$\nu = 0.1$	Yes	SR
IN2	$v_y = -\sin(t)$	$\rho = 1.0$		TR
IN3	$Pr = \sin(t)$			STR
IN4	$u_x = \sin(2t) \cos(y)$	$\nu = 0.1$	Yes	SR
IN5	$v_y = -\sin(2t) \cos(x)$	$\rho = 1.0$		STR
	$Pr = \sin(2t)(\cos(2x) + \cos(2y))$			
PRES	$u_x = e^{-0.2t} \sin(x) \cos(y)$ $v_y = -e^{-0.2t} \cos(x) \sin(y)$ $Pr = e^{-0.4t}(\cos(2x) + \cos(2y))$	$\nu = 0.1$ $\rho = 1.0$	Yes	SR
CON	$u_x = e^{-0.1t} \sin(x) \cos(y)$ $v_y = -e^{-0.1t} \cos(x) \sin(y)$ $Pr = \frac{3}{80}e^{-0.2t}(\cos(2x) + \cos(2y))$	$\nu = 0.05$ $\rho = 1.5$	Yes	SR
VIS	$u_x = e^{-t} \sin(x) \cos(y)$ $v_y = -e^{-t} \cos(x) \sin(y)$ $Pr = \frac{3}{40}e^{-2t}(\cos(2x) + \cos(2y))$	$\nu = 0.5$ $\rho = 0.3$	Yes	SR

## 5 RESULTS

### 5.1 Taylor Green Vortex (TGV)

In this benchmark, all the terms in the N-S equations are having equal weights. TGV constitutes the simplest flow for which a turbulent energy cascade can be observed numerically.

The rationale for choosing TGV as an initial test case for KratosCFD VMS monolithic solver was two-fold: Firstly, the TGV is a well-established reference in the literature. Secondly, the physics of the flow field and the ease of BC constitute and excellent benchmark

for VMS implementations. Three simulations were performed using TGV for different refinement approaches as listed in table 2 (TGV1, TGV2 and TGV3). For TGV1, spatial refinement was performed having a very fine time step. The reason was to minimize the time discretization error and test the spatial discretization. For TGV2, temporal refinement was performed having a very fine mesh to minimize space discretization error and test the temporal discretization.

Finally TGV3, both space and time were refined sequentially to check the discretization in space and time. The third approach, TGV3, was used because both time and space discretization have a theoretical second order convergence. In this case of having equal orders, convergence studies can be performed for space and time simultaneously.

The results produced by KratosCFD for the presented test cases are shown in figure 2. The figure shows the observed order of accuracy ( $p$ ) versus refinement. As can be seen from the figure, a second order of accuracy is observed which complies with the theoretical order of accuracy.

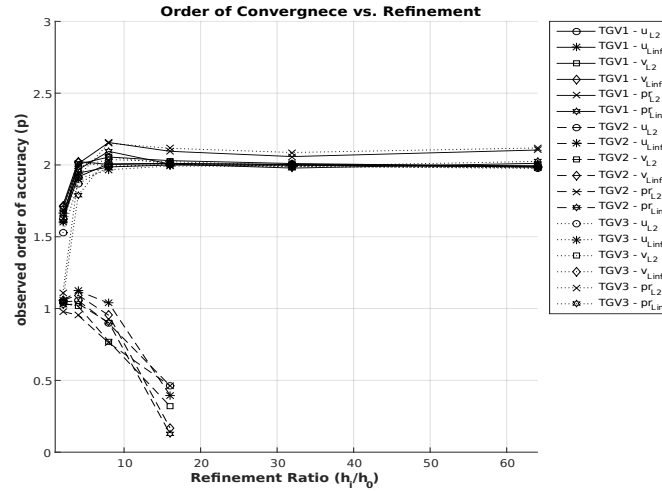


**Figure 2:** Observed order of accuracy for Taylor-Green Vortex (TGV Benchmark)

## 5.2 Inertia dominated flow (IN)

From the first test case, it can be concluded that the code performance is acceptable. But TGV2 showed a deviation from the expected performance. For time refinement only, the code performance is unexpected. Consequently, this case study was designed to only test the inertial term in the N-S equations. The case study presented shows two different approaches: Firstly, the manufactured solution fields are only time dependent functions as in cases IN1, IN2 and IN3. Secondly, the manufactured solution fields have time and



space dependency as in cases IN4, IN5. In both cases, the time derivative term of the unsteady N-S equations is dominating. Contributions from all other terms are zero in the first case and negligible in the second case.

The code's performance for a time dependent solution is evaluated in test cases IN1 to IN5. Figure 3 shows a reasonable results for a spaces only refinement (IN1) in a time driven solution where there is no clear convergence behavior.

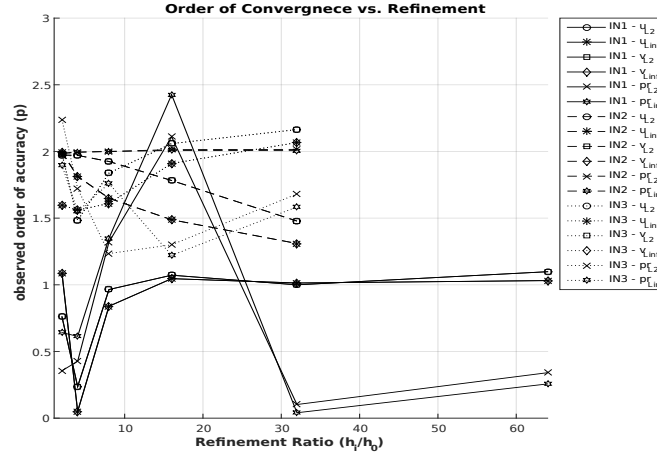


**Figure 3:** Observed order of accuracy for Inertia dominated flow (IN Benchmark)

Consequently, case IN2 was performed, where the simulation was performed with a time refinement at the finest mesh. Figure 3 shows that a second order of accuracy is observed for the pressure field (IN2). Whereas for the velocity field, the observed order of accuracy is between 1.5 and 2 for some simulations. The performance of the code is not as expected for a time-only dependent solution. Consequently, IN3 is performed having a space-time refinement. Figure 3 shows a second order of accuracy for the velocity field, but an order between 1.5 and 2 for the pressure field (IN3). From cases IN1, IN2 and IN3, it can be concluded that there is some sort of instability in Kratos VMS formulation for cases of only time-dependent solutions.

This observation is investigated more by cases IN4 and IN5. In this approach the time derivative of the N-S equations is high compared to the minor contribution from the space derivative. Figure 4 show an order of convergence slightly below 2 for all the fields. Consequently, it can be safely said that the code has a second order of accuracy for time derivatives.

### 5.3 Pressure dominated flow (PRES)

The purpose of this simulation is to numerically check the code's accuracy if the pressure term in the N-S equations is dominating the flow. From previous cases, it can be

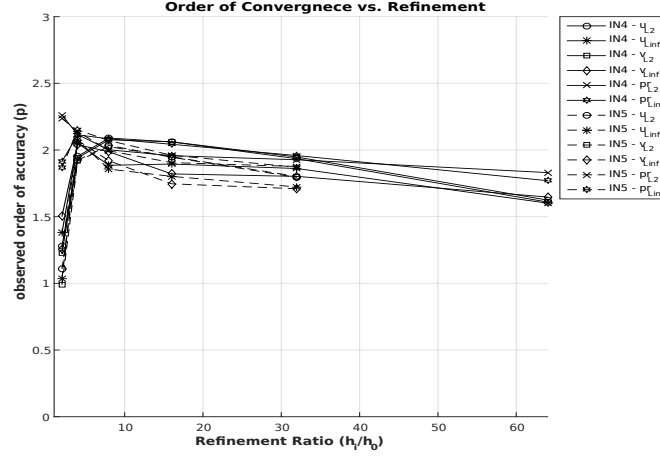


**Figure 4:** Observed order of accuracy for Modified Inertia dominated flow (IN4 and IN5 Benchmark)

concluded that for the Kratos code, spatial and temporal discretization are correlated in some sense and solution accuracy is more sensitive for mesh refinement than for time refinement. Consequently, only mesh refinement simulations were performed for this case.

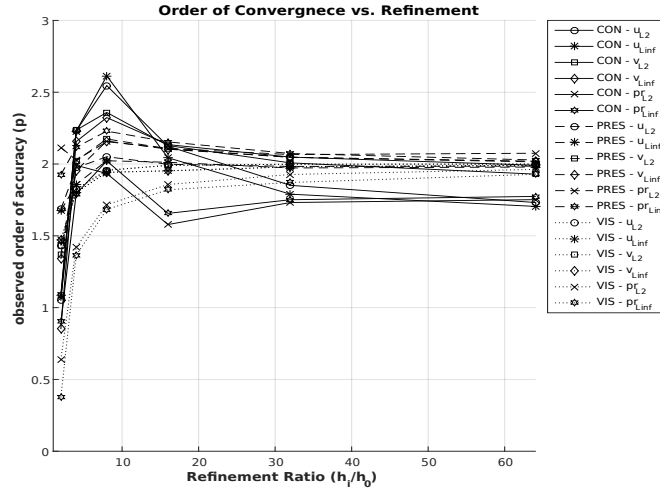


**Figure 5:** Observed order of accuracy for pressure, convection and viscous dominated flows (PRES, CON and VIS Benchmark)

PRES simulation is performed with spatial refinement. From figure 5, it can be concluded that the observed order of accuracy in both cases is almost second order.

#### 5.4 Convection dominated flow (CON)

The purpose of this simulation is to numerically check the code's accuracy if the Convection term in the N-S equations is dominating the flow. It can be concluded that the observed order of accuracy is approaching second order as shown in figure 5.

#### 5.5 Viscous dominated flow (VIS)

The purpose of this simulation is to numerically check the code's accuracy if the Viscous term in the N-S equations is dominating the flow. Only mesh refinement simulations are performed for this case. It can be concluded that the observed order of accuracy is near second order as shown in figure 5.

### 6 CONCLUSIONS

The presented test cases are not meant to test the physical efficiency of the code but the numerics. The development of the test cases is code dependent. For example, a code that performs as expected from the first test case (TGV) can be considered verified. Whereas, verifying Kratos has required more than the base test. While performing the TGV2 simulation, the code performance was completely unexpected. Therefore, more rigorous tests were required. Four test cases are developed to examine the code performance under different numerical testing by numerical exploit the effect of each of the four terms in the N-S equations. From the inertia dominated terms, it can be safely concluded that there is a time-space correlation in the discretized space. In other words, time-dependent only solutions such as IN1 cannot be handled by the code. This is not a disadvantage of the code but it is part of the formulation used for the VMS element. All test cases showed an observed second order accuracy. Therefore, the observed order of accuracy matches the theoretical order of accuracy. Finally, it can be safely said that the VMS monolithic solver is verified in KratosCFD.

### REFERENCES

- [1] J. Franke, A review of verification and validation in relation to CWE. *The Fifth International Symposium on Computational Wind Engineering (CWE2010)*. North Carolina, USA, 2010.
- [2] R. Jauregui and F. Silva, Numerical Validation Methods, Numerical Analysis - Theory and Application. n, Prof. Jan Awrejcewicz (Ed.), ISBN: 978-953-307-389-7, In-Tech. Available from: <http://www.intechopen.com/books/numerical-analysis-theory-and-application/numerical-validation-methods>.
- [3] A. Abodonya, Validation of Wind-Structure Interaction Simulations for Pneumatic Inflatable Structures. *Master Thesis, Technical University of Munich*. Germany, 2014.

- [4] A. Abodonya, H. Alsofi, R. Wüchner and K. Bletzinger, From Experimental Wind Tunnel to Wind-Structure Interaction Simulations of a Shell Structure. *Resilient Infrastructure (CSCE2016)*. London, Ontario, Canada, 2016.
- [5] R. Fisch, Code verification of partitioned FSI environments for lightweight structures. *PhD Thesis, Technical University of Munich*. Germany, 2014.
- [6] W. L. Oberkampf and C. J. Roy, Verification and Validation in Scientific Computing. *Cambridge University Press*. 2010.
- [7] P. Knupp and K. Salari, Verification of Computer Codes in Computational Science and Engineering. *CHAPMAN & HALL/CRC*. 2003.
- [8] P. J. Roache, Verification and Validation in Computational Science and Engineering. *hermosa publishers*. 1998.
- [9] KRATOSMulti-physics, GitHub repository, <https://github.com/KratosMultiphysics/Kratos>. 2017.
- [10] R. Codina, Stabilized finite element approximation of transient incompressible flows using orthogonal subscales. *Computer methods in applied mechanics and engineering*. 2002.
- [11] J. Cotella, Applications of turbulence modeling in civil engineering. *PhD Thesis, Universitat Politècnica de Catalunya*. Spain, 2016.
- [12] G. I. Taylor and A. E. Green, Mechanism of the Production of Small Eddies from Large Ones. *Proceedings of the Royal Society of London. Series A, Mathematical and Physical Sciences*. Vol. 158, No. 895, pp. 499-521, 1937.
- [13] A. J. Chorin, Numerical solution of the NavierStokes equations. *Math. Comp.*, 22, 745762, 1968.